

SIMULATION OF A MULTIMATERIAL MODEL FOR MODIFIED AUXETIC STRUCTURES

ALEXANDER ENGEL*, ANNE JUNG

Helmut Schmidt University/University of the Federal Armed Forces Hamburg, Protective Systems, Holstenhofweg 85, 22043 Hamburg, Germany

* corresponding author: a.engel@hsu-hh.de

ABSTRACT. Auxetic structures, which is a term used to describe materials with a negative Poisson’s ratio, show beneficial properties like a low density, a high energy absorption capacity and an increased indentation resistance. This enables applications in many fields, such as aerospace and sports industries. Given their potential, many studies have already been conducted. Previously, the geometry of a selected auxetic re-entrant structure was optimized to maximize its mass-specific energy absorption capacity for ideal usage in lightweight applications. Moreover, a homogeneous material was used, whereas the combination of multiple materials could drastically increase the performance of such structures. Hence, in this study the use of two different materials combined into a modified re-entrant structure is investigated via Finite Element simulation. The Poisson’s ratio could thus be improved, which leads to a more pronounced and longer lasting auxetic effect.

KEYWORDS: Auxetic metamaterials, multi-material structure, lightweight, energy absorption.

1. INTRODUCTION

Auxetic materials are defined by a negative Poisson’s ratio ν , which describes the change in volume from the negative ratio between the transversal strain ε_t and the longitudinal strain ε_l under uniaxial loading [1].

$$\nu = -\frac{\varepsilon_t}{\varepsilon_l}. \quad (1)$$

The deformation behavior is shown schematically in Figure 1 for an auxetic and a non-auxetic material under uniaxial tension as well as uniaxial compression.

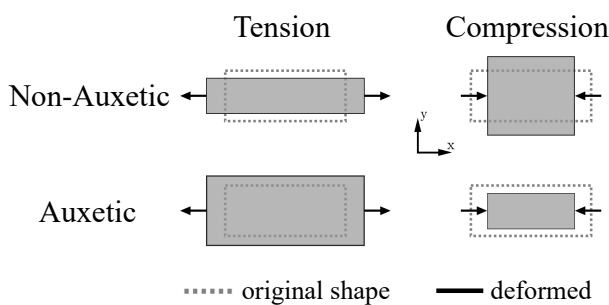


FIGURE 1. Deformation behavior of auxetic and non-auxetic structures under uniaxial loading.

Additionally, auxetic materials have several advantages over conventional materials, making them central to many current research projects [2, 3]. These include an increased thermal shock resistance [4], a higher fracture toughness [5], an increased penetration resistance [6, 7], a high volume-specific energy dissipation [8] and a low density, enabling applications in many fields, such as ballistic and explosion protection, as energy absorbers, or in lightweight construc-

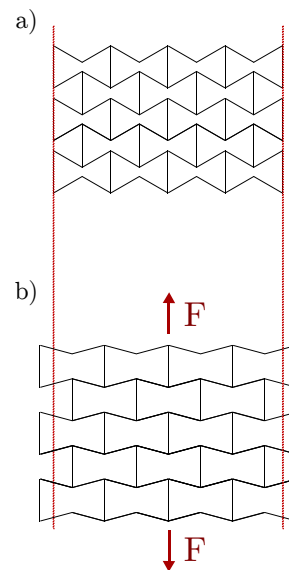


FIGURE 2. 2D auxetic re-entrant structure in a) non-deformed and b) deformed stage.

tion [9, 10]. Other applications include piezoelectric composites, medical applications such as stents and bandages, and sports applications through reduced impact forces and friction [10, 11].

Several classes of auxetic structures can be distinguished. Starting with two-dimensional (2D) structures and the most widespread class, the re-entrant structure [2, 12]. The deformation mechanism of the re-entrant structure is relatively simple to understand and is shown schematically in Figure 2. These, as well as other 2D structures, are easily expandable into the third dimension and exhibit unidirectional auxetic behavior [2, 13]. By applying a load, the struts of

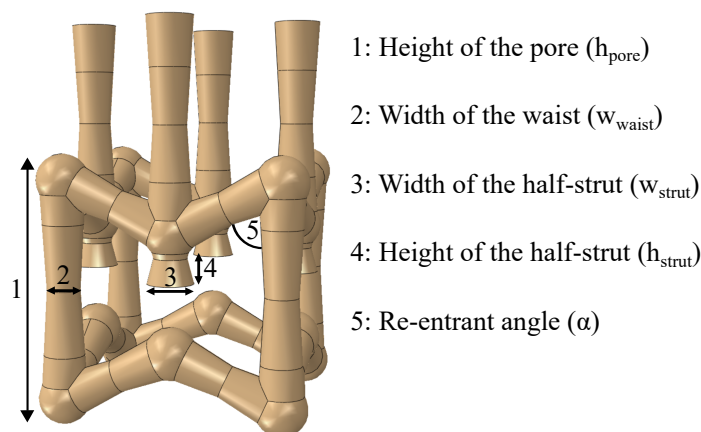


FIGURE 3. Unit cell of a modified auxetic re-entrant structure.

the structures rotate, stretch and bend, resulting in a lateral volume increase and thus auxetic behavior [2, 14, 15].

Some of these characteristics could be improved even further by the utilization of a non-homogeneous material for the auxetic structure, since the targeted use of varying stiffnesses for different structural components is expected to have an impact onto the deformation and thus the Poisson's ratio.

2. MATERIALS AND METHODS

2.1. GEOMETRY

The studied structure is a three dimensional re-entrant structure, which has been modified in order to maximize its mass-specific energy absorption capacity for ideal usage in lightweight construction by Bronder et al. [9]. Through the modification, an additional half strut was introduced to the re-entrant geometry. Figure 3 shows the different structural parameters that have been optimized.

The optimized values of these geometric parameters are shown in Table 1.

Structural parameter	Optimized value
h_{pore}	7.29 mm
w_{waist}	0.56 mm
h_{strut}	1.66 mm
w_{strut}	0.78 mm
α	65.61 Å

TABLE 1. Optimized geometry parameters for the modified auxetic re-entrant structure [9].

For the analysis, a total of 27 ($3 \times 3 \times 3$) unit cells were used. This enables one unit cell in the center of the structure to be mostly unaffected by boundary effects, whilst still keeping the necessary time for each simulation manageable.

2.2. MATERIALS

In order to further improve upon this structure, an effort has been made to move away from a homogeneous material and instead introduce materials with a distinct variation in terms of their stiffness. For that purpose, the horizontal struts were set to be austenitic and the vertical struts were assigned a martensitic material model thus still avoiding major discrepancies in density and composition by sticking to different variants of steel. The martensitic struts are introduced in order to avoid bending of the outer struts which would limit the overall auxetic effect and thus resulting in a lower Poisson's ratio. Hence this bending is avoided by utilizing a material with a relatively high stiffness. However, since the austenitic parts have a lower stiffness than the martensitic parts, it is expected, that the horizontal struts can still flex and hinge in order to get auxetic deformation in the first place, hence leading to a more pronounced auxetic effect when compared to a similar structure with a homogeneous material.

2.3. SIMULATIONS

All simulations were done using the Finite Element software ABAQUS® (Dassault Systèmes, Vélizy-Villacoublay, France). Both materials were assigned an isotropic, elastic-plastic material model. The material data of each bulk material is shown in Table 2.

Parameter	Value
$E_{Austenite}$	220 MPa
$E_{Martensite}$	210 MPa
$\rho_{Austenite}$	7.9 g cm ⁻³
$\rho_{Martensite}$	7.8 g cm ⁻³
$\nu_{Austenite}$	0.300
$\nu_{Martensite}$	0.283

TABLE 2. Material data of the bulk materials for austenite and martensite, including the Young's moduli E , the densities ρ and the Poisson's ratios ν .

Furthermore, for both austenite and martensite, a ductile damage model was introduced with an equivalent plastic strain at the onset of damage of 0.3 and 0.01 respectively. The loading was applied by subjecting a rigid body plate to displacement-controlled compression, which was coupled to the structure via a general contact. A hard contact was defined between the two plates and the auxetic structure in the normal direction, which means that the surfaces of the structure and the two plates cannot be penetrated. In the tangential direction, a friction coefficient of 0.1 was defined [16]. In order to evaluate the Poisson's ratio, the longitudinal and the transversal strain were measured. The longitudinal strain was taken from the load point and the transversal strain was taken from the average strain of the nodes within the corners of the outer unit cells of the middle layer of the structure. The Poisson's ratio was also evaluated in both principal planes perpendicular to the load axis, however, given the symmetric nature of the structure and the uniaxial loading conditions, both lead to the same results. Hence, from this point onward the Poisson's ratio will only be shown for one principal plane. The loading conditions as well as the nodes used for evaluation are shown in Figure 4. In order to achieve a sufficient accuracy during the simulations, the mesh was found to require at least two elements across the width of one strut. Hence, the mesh size was set to be half of the width of a strut. Furthermore, modified quadratic tetrahedral elements (C3D10M) were used for the mesh in order to achieve an improved contact properties and good performance over the complete range of deformation [16].

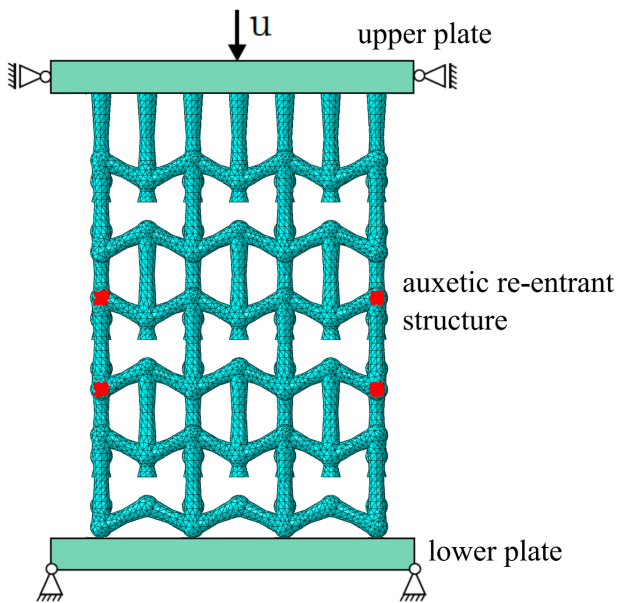


FIGURE 4. Loading conditions for the compressive load applied to the modified auxetic re-entrant structure with the highlighted nodes (red) being used to evaluate the Poisson's ratio.

For the purpose of studying the effect of introduc-

ing multiple materials for the same structure, quasi-static simulations were performed for a homogeneous austenitic structure, a homogeneous martensitic structure as well as the combined multimaterial structure. The unit cells of each structure is shown in Figure 5.

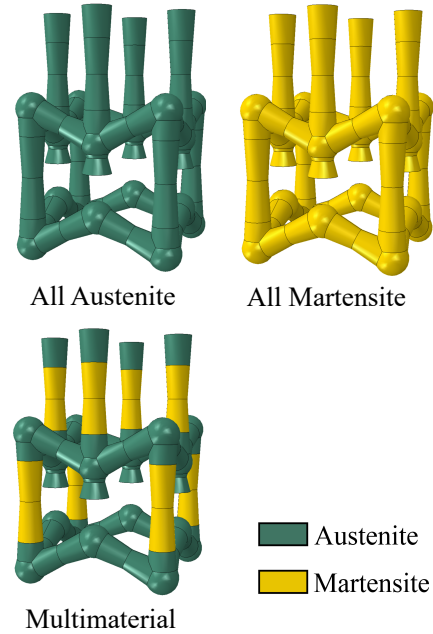


FIGURE 5. Unit cells of the multimaterial, homogeneous austenitic and homogeneous martensitic structure.

3. RESULTS

In order to evaluate the auxetic behavior of the different structures, the Poisson's ratio will serve as the decisive parameter. Hence, the strain along the compressive load axis will be evaluated as the longitudinal strain $\varepsilon_{Longitudinal}$ and the strain perpendicular to the load axis as the transversal strain $\varepsilon_{Transversal}$ in order to calculate the Poisson's ratios according to Equation 1. Thus, an increase in the negative amount of the Poisson's ratio correlates to a more pronounced auxetic effect and as such an increased performance. The Poisson's ratios for each of the different structures are shown up until 12% strain in Figure 6.

Immediately, a difference between the three structures can be noticed, solely based on their material combination. Whilst the homogeneous martensitic structure shows barely any auxetic deformation, the other two structures show promising results. The reason for the martensitic structure showing barely any auxetic deformation is based on the very high stiffness of the material. Since it is necessary for auxetic structures to flex and bend certain parts, the high stiffness counteracts this deformation. Additionally, failure occurs at a very low strain, also resulting in an attenuation of the auxetic effect. Hence, the homogeneous austenitic structure shows a stronger auxetic effect because of its increased ductility and

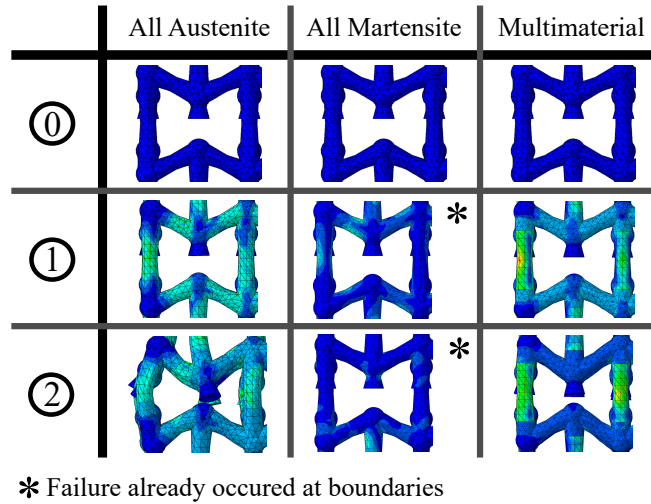
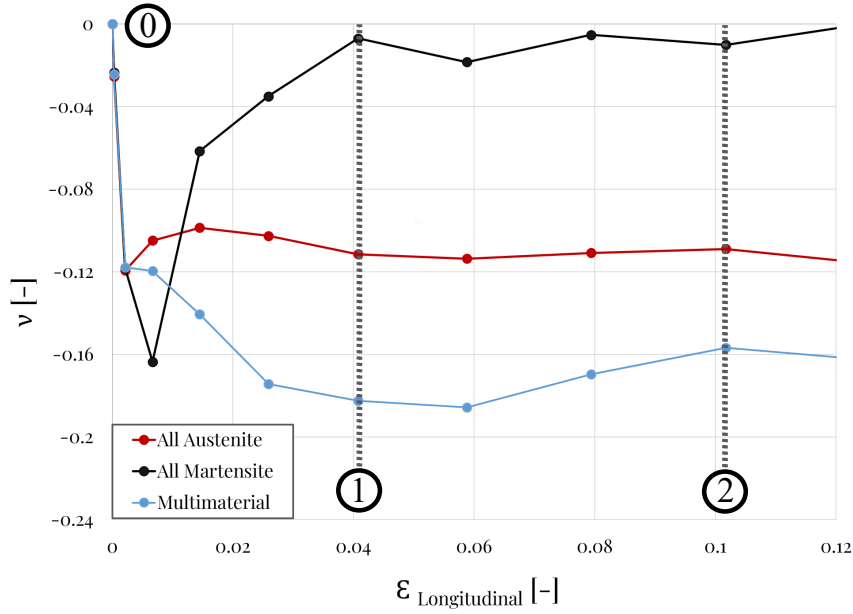


FIGURE 6. Poisson's ratio of the modified auxetic re-entrant structure for the homogeneous austenitic (All Austenite), homogeneous martensitic (All Martensite) and combined multimaterial (Multimaterial) structure.

the ability to bend certain parts of the structure due to a lower stiffness. However, the most promising results in terms of the Poisson's ratio are shown by the combined multimaterial structure. The combination of both materials leads to less buckling of the outer struts due to the martensitic parts, whilst still allowing for enough ductile deformation and bending caused by the horizontal austenitic struts.

The Poisson's ratios of each structure at different strain points, according to Figure 6, are shown in Table 3. An increase of roughly 50% in terms of the negative amount of the average Poisson's ratio can be noticed from the homogeneous austenitic structure to the multimaterial structure. This significant improvement could already be achieved without optimizing the materials used for the model. Utilizing carefully selected materials with varying stiffness can

certainly help to improve the performance of complex auxetic structures and make them more suitable for application.

Material setup	Poisson's ratio [-]
All Austenite	① -0.112
	② -0.109
All Martensite	① -0.007
	② -0.011
Multimaterial	① -0.183
	② -0.157

TABLE 3. Poisson's ratios of the modified auxetic structure for different material setups.

4. CONCLUSION

First steps have been made towards the improvement of a selected auxetic structure by introducing multiple materials to an auxetic structure. Hence, austenitic and martensitic parts were introduced to a modified auxetic re-entrant structure, whereby martensite has a significantly higher stiffness than austenite thus avoiding buckling of the outer struts. However, the austenitic parts still allow for flexure to get auxetic deformation in the first place. Thus, the deformation behavior of these structures has been analyzed and the impact of different geometry parameters on the Poisson's ratio has been studied. It was shown, that the use of selected combinations of materials within the same structure can lead to serious improvements in the overall deformation behavior, and as such the Poisson's ratio, but also the application-oriented performance. In the future, it will be necessary to fabricate samples in order to compare the results from the simulations to actual experiments.

REFERENCES

- [1] X. Hou, V. V. Silberschmidt. *Mechanics of Advanced Materials*, chap. Metamaterials with negative Poisson's ratio: A review of mechanical properties and deformation mechanisms, pp. 155–179. Springer, 2015. https://doi.org/10.1007/978-3-319-17118-0_7
- [2] N. Novak, M. Vesenjak, Z. Ren. Auxetic cellular materials – a review. *Strojniški vestnik-Journal of Mechanical Engineering* **62**(9):485–493, 2016. <https://doi.org/10.5545/sv-jme.2016.3656>
- [3] T. Fíla, P. Koudelka, J. Falta, et al. Dynamic impact testing of cellular solids and lattice structures: Application of two-sided direct impact Hopkinson bar. *International Journal of Impact Engineering* **148**:103767, 2021. <https://doi.org/10.1016/j.ijimpeng.2020.103767>
- [4] T.-C. Lim. Thermal stresses in auxetic plates and shells. *Mechanics of Advanced Materials and Structures* **22**(3):205–212, 2015. <https://doi.org/10.1080/15376494.2012.727203>
- [5] R. S. Lakes. Design considerations for materials with negative Poisson's ratios. *Journal of Mechanical Design* **115**(4):696–700, 1993. <https://doi.org/10.1115/1.2919256>
- [6] C. Qi, A. Remennikov, L.-Z. Pei, et al. Impact and close-in blast response of auxetic honeycomb-cored sandwich panels: Experimental tests and numerical simulations. *Composite structures* **180**:161–178, 2017. <https://doi.org/10.1016/j.compstruct.2017.08.020>
- [7] S. Yang, C. Qi, D. Wang, et al. A comparative study of ballistic resistance of sandwich panels with aluminum foam and auxetic honeycomb cores. *Advances in Mechanical Engineering* **5**:589216, 2013. <https://doi.org/10.1155/2013/589216>
- [8] M. Bianchi, F. L. Scarpa, C. W. Smith. Stiffness and energy dissipation in polyurethane auxetic foams. *Journal of Materials Science* **43**(17):5851–5860, 2008. <https://doi.org/10.1007/s10853-008-2841-5>
- [9] S. Bronder, F. Herter, A. Röhrig, et al. Design study for multifunctional 3d re-entrant auxetics. *Advanced Engineering Materials* **24**(1):2100816, 2021. <https://doi.org/10.1002/adem.202100816>
- [10] X. Yu, J. Zhou, H. Liang, et al. Mechanical metamaterials associated with stiffness, rigidity and compressibility: A brief review. *Progress in Materials Science* **94**:114–173, 2018. <https://doi.org/10.1016/j.pmatsci.2017.12.003>
- [11] Z. Wang, H. Hu. Auxetic materials and their potential applications in textiles. *Textile Research Journal* **84**(15):1600–1611, 2014. <https://doi.org/10.1177/0040517512449051>
- [12] F. Scarpa, P. Panayiotou, G. Tomlinson. Numerical and experimental uniaxial loading on in-plane auxetic honeycombs. *The Journal of Strain Analysis for Engineering Design* **35**(5):383–388, 2000. <https://doi.org/10.1243/0309324001514152>
- [13] C. Körner, Y. Liebold-Ribeiro. A systematic approach to identify cellular auxetic materials. *Smart Materials and Structures* **24**(2):025013, 2014. <https://doi.org/10.1088/0964-1726/24/2/025013>
- [14] S. Bronder, M. Adorna, T. Fíla, et al. Hybrid auxetic structures: Structural optimization and mechanical characterization. *Advanced Engineering Materials* **23**(5):2001393, 2021. <https://doi.org/10.1002/adem.202001393>
- [15] X. Ren, R. Das, P. Tran, et al. Auxetic metamaterials and structures: a review. *Smart materials and structures* **27**(2):023001, 2018. <https://doi.org/10.1088/1361-665X/aaa61c>
- [16] M. Smith. *ABAQUS/Standard User's Manual, Version 6.9*. Dassault Systèmes Simulia Corp, United States, 2009.